ACS Photonics

Letter

Cite This: ACS Photonics 2018, 5, 2978−2982

Raman Enhancement of Blood Constituent Proteins Using Graphene

Shengxi Huang,*[,†,‡,#] Rishikesh Pandey,*[,§,#] Ishan Barman,[∥,⊥] Jing Kong,*[,†] and Mildred Dresselhaus[†]

[†]Department of Electrical Engineering and Computer Sciences, Massachusetts Institute of Technology, Cambridge, Massachusetts 02139, United States

[‡]Department of Electrical Engineering, The Pennsylvania State University, University Park, Pennsylvania 16802, United States

[§]Connecticut Children's Innovation Center, University of Connecticut School of Medicine, Farmington, Connecticut 06032, United States

[∥]Department of Mechanical Engineering, Johns Hopkins University, Baltimore, Maryland 21218, United States

[⊥]Department of Oncology, Johns Hopkins University, Baltimore, Maryland 21287, United States

Supporting Information

ABSTRACT: Raman spectroscopy has drawn considerable attention in biomedical sensing due to the promise of label-free, multiplexed, and objective analysis along with the ability to gain molecular insights into complex biological samples. However, its true potential is yet to be realized due to the intrinsically weak Raman signal. Here, we report a simple, inexpensive and reproducible signal enhancement strategy featuring graphene as a substrate. Taking key blood constituent proteins as representative examples, we show that Raman spectra acquired from biomacromolecules can be reproducibly enhanced when these molecules are placed in contact with graphene. In particular, we demonstrate that hemoglobin and albumin display significant, but different, enhancement with the enhancement factor depending on the Raman modes, excitation wavelengths, and analyte concentrations. This technique offers a new strategy for label-free biosensing owing to the molecular fingerprinting capability, signal reliability, and simplicity of the enhancement method.

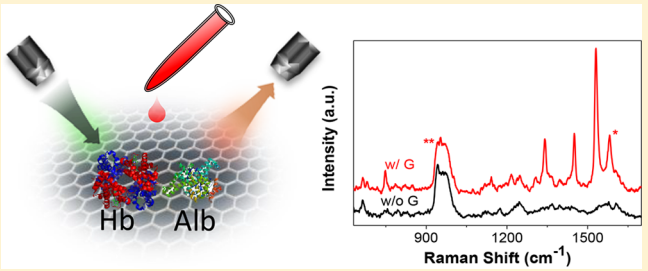

KEYWORDS: *graphene, Raman spectroscopy, blood analytes, label-free sensing, GERS*

In recent decades, photonic sensors have drawn considerable attention in rapid identification and quantification of bioanalytes.[1,2] Powered by their intrinsic molecular specificity and multiplexing capability, optical spectroscopy sensors, in particular, appear to be the most promising among various biosensing techniques. Of note, Raman spectroscopy provides quantitative and molecular fingerprint information non-invasively and thus holds great promise as a diagnostic tool.[3] However, the cross section of Raman scattering is typically very low, which limits its diagnostic sensitivity. For applications in clinical diagnosis, Raman measurements must be highly sensitive, simple, and reproducible. Therefore, an effective method to enhance the Raman scattering signals is highly desirable. Several strategies have been investigated to enhance Raman signal thereby increasing the detection sensitivity.[4−7] Notably, the widespread adoption of surface enhanced Raman spectroscopy (SERS), which provides immense enhancement attributed to both plasmonic and chemical mechanisms, is impeded by unpredictable variations in acquired spectra that has led to the theorization of a "SERS-uncertainty principle".[8]

Graphene-enhanced Raman scattering (GERS) is a technique of Raman enhancement which uses graphene as a substrate.[9−12] We have previously shown that the Raman signals of many organic molecules are enhanced when placed on graphene surface.[9,10] The signal enhancement by graphene has been primarily attributed to the charge transfer between graphene and the analyte. Factors that determine enhancement include graphene Fermi level, energy levels of the analyte, namely highest occupied molecular orbital (HOMO) and lowest unoccupied molecular orbital (LUMO), analyte molecular structure, and laser excitation wavelength.[10] Although GERS has been observed previously, almost all the studies have been limited to small molecules.[9,12,13] However, to the best of our knowledge, this is the first investigation which reports graphene mediated Raman signal enhancement from complex macromolecules, such as, hemoglobin and albumin.

This enhancement method is different from the conventional SERS, which exploits the plasmonic nanostructure to increase the effective local field in the vicinity of the substrate. GERS, on the other hand, has the advantages of high reproducibility and uniformity of signal enhancement, which are essential in enriching the reliability of biosensing and reducing false alarms in clinical applications including disease

Received: April 10, 2018
Published: July 9, 2018

DOI: 10.1021/acsphotonics.8b00456
ACS Photonics 2018, 5, 2978−2982

diagnosis and treatment response monitoring. In addition to signal amplification, graphene aids in suppression of fluorescence from surface-adsorbed molecules,[14] and consequently also reduces variation due to bleaching, both of which are highly desirable attributes for sensitive Raman measurements. Owing to these salient features, we hypothesize that GERS may offer a reliable and convenient method for biosensing. Hence, our objective in this study was to test the feasibility of GERS in detecting biomolecules. We selected two proteins found abundantly in the blood, hemoglobin (Hb) and albumin (Alb) based on their unique structure and functional importance.

An illustration of GERS measurements is shown in Figure 1. Here, the blood analytes are placed in contact with monolayer graphene. The excitation laser shines on the biomolecules, and the scattered signal is measured using a Raman spectrometer. In the current study, monolayer graphene is fabricated through mechanical exfoliation and placed on the Si/SiO_2 substrate. The thickness of SiO_2 is chosen to be 300 nm to achieve the best visibility of monolayer graphene flakes and also to obtain sufficient Raman signals of analytes without graphene for ready evaluation of GERS enhancement factor. In order to obtain reliable GERS results, we ensured that the graphene substrate is free of any impurity and the Raman signals are specifically obtained on clean graphene monolayer without any tape residue. In this context, the schematic of mechanical exfoliation of graphene along with atomic force microscopy and Raman spectroscopy characterization results of monolayer graphene are provided in Supporting Information (SI). An optical microscope image of the exfoliated graphene sample is shown on the left panel of Figure 1. In Figure 1, the portion highlighted in the yellow dotted regions shows graphene monolayer. Following the preparation of graphene substrates, the aqueous solutions of Hb and Alb with different concentrations were prepared. The Si/SiO_2 substrates with graphene flakes were soaked in the Hb solution for 2 h, followed by instantaneous blow drying. Next, we performed Raman measurement on both the region of the samples with graphene and the region on bare Si/SiO_2 adjacent to graphene flakes, using two excitation wavelengths in the visible range, 532 and 633 nm, as shown in Figure 1. The detailed sample preparation and measurement methods are provided in SI.

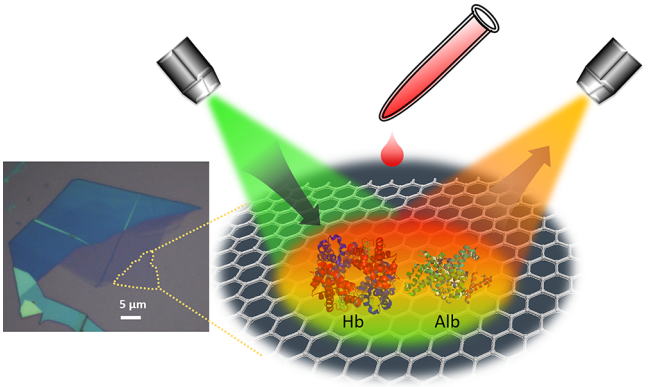

Figure 1. Illustration of the GERS measurement. Left: optical microscopic image of a graphene flake. The yellow dotted region highlights the monolayer graphene. Right: GERS measurement. The biomolecules, Hb and Alb, are first dissolved in water, then graphene substrate is soaked in the solution, resulting in adsorption of Hb and Alb on graphene substrate. Laser is illuminated on the sample, and Raman scattered light is collected and analyzed by the Raman spectrometer.

The Raman spectra of Hb on graphene and on bare Si/SiO_2 substrates at 532 nm excitation are displayed in Figure 2a. As can be seen, the Raman signal of Hb on graphene is enhanced as compared to the signal collected on the bare Si/SiO_2 substrate. Many signature peaks of Hb, such as 670, 753, 1224, 1376, and 1638 cm^{-1},[15,16] are enhanced when recorded on the graphene substrate. The prominent bands include heme-related features, such as the 670, 753, and 1638 cm^{-1} belonging to the porphyrin skeletal modes, and the 1376 cm^{-1} mode that represents pyrrole half ring stretching. Of note, not all the modes are enhanced, and the enhancement factors are observed to vary from mode to mode. Furthermore, in order to understand the impact of resonance (or lack thereof) on graphene signal enhancement, we carried out the Raman measurement at 633 nm excitation as presented in

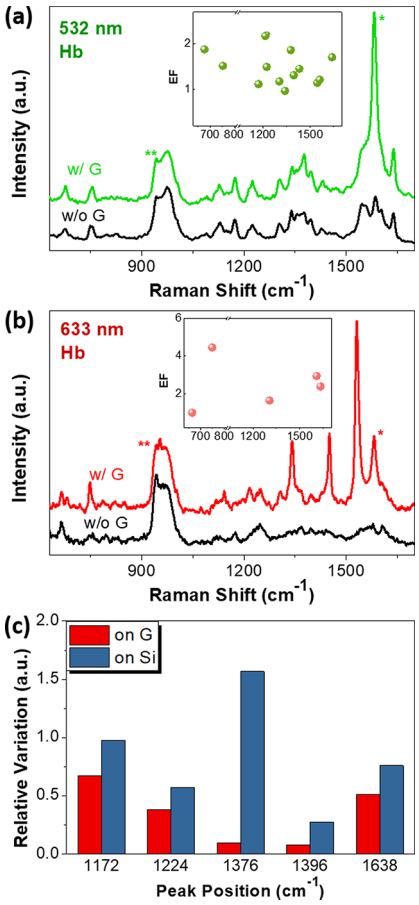

Figure 2. Raman spectra of Hb in contact with and in absence of graphene measured under 532 (a) and 633 (b) nm excitation laser wavelengths, respectively. The green and red spectra show the Raman spectra of Hb on graphene, and the black spectra show the spectra of Hb on bare Si/SiO_2 substrate without graphene. The graphene G bands at around 1582 cm^{-1} are labeled with "*", and the second-order modes of Si substrate are labeled with "**". The spectra are normalized by the Si Raman mode. Insets of (a) and (b) present the enhancement factor (EF) of GERS for different Raman modes under 532 and 633 nm laser, respectively. The concentration of the Hb was 7.5 mg/mL. (c) Relative variation of the Raman peak intensities measured on SiO_2/Si and graphene substrates for 7.5 mg/mL Hb, under 532 nm laser excitation.

DOI: 10.1021/acsphotonics.8b00456
ACS Photonics 2018, 5, 2978−2982

Figure 2b. It can be observed that graphene-mediated enhancement occurs for 633 nm laser excitation as well. However, under 532 nm excitation, the Raman signal of Hb on bare substrate is observable, because the HOMO−LUMO gap of Hb is in resonance with 532 nm laser. On the other hand, due to the nonresonant condition with 633 nm excitation, the Raman signal is not obvious for the same Hb solution on bare Si/SiO_2 substrate. The enhancement effect at 633 nm is more obvious than 532 nm excitation: clear Raman features of Hb on graphene are observed for 633 nm excitation, while no obvious peaks are noticed for the specimen studied in the absence of graphene monolayer.

One can readily compute the GERS enhancement factors, which are shown in the insets of Figure 2a,b for 532 and 633 nm laser excitations, respectively. As can be seen, different Raman modes have different enhancement factors. For 532 nm laser excitation, 753 cm^{-1} mode has the enhancement factor of around 1.5, 1376 cm^{-1} mode has the enhancement of around 2.0, 1638 cm^{-1} has the enhancement of around 1.7, while the other modes have enhancement slightly more than 1. The GERS enhancement factor smaller than 5 is not uncommon and has been observed in a number of organic molecules we studied before.[10] Few examples of such molecules and related discussions are provided in the SI. For 633 nm laser, the overall enhancement is stronger than 532 nm excitation. There is strong enhancement for the heme modes, 1340, 1450, and 1530 cm^{-1}, but these modes have no obvious enhancement for 532 nm laser. For the spectral band at 753 cm^{-1}, the enhancement is more than 4 under 633 nm laser, while it is only about 1.5 under 532 nm laser. Such an enhancement dependence on Raman modes has also been observed in previous works for many organic molecules such as phthalocyanine molecules,[10,17,18] and can be attributed to the different Raman resonance conditions with varying laser excitation energies, which has been theoretically proved using third-order perturbation theory in Raman scattering.[19] We also observed that the overall Hb Raman signal was stronger on monolayer graphene as compared to when placed on multilayer graphene (Figure S4 in SI).

Moreover, we also observed that the Raman signal is more reproducible on graphene than on Si/SiO_2 substrate. During the experiment, for each sample under the same experiment conditions, we performed Raman measurements on 9 spatial locations on both graphene and Si/SiO_2 substrates. We then calculated the relative intensity variations of the Raman peaks on both graphene and on Si/SiO_2 substrates. Figure 2c shows the relative variations of different peaks for Hb of 7.5 mg/mL concentration acquired under 532 nm excitation. As evident from the figure, for all peaks, the Raman spectra variations on Si/SiO_2 substrate are significantly larger than on graphene substrate. This smaller variation on graphene is also observed across the Hb concentrations and excitation wavelengths. This observation clearly indicates the advantage of using graphene as the Raman substrate: providing uniform, reproducible and reliable signal. Such uniformity and reproducibility may be ascribed to the imperfection-free, flat, and chemically inert surface of graphene.[9]

Additionally, we investigated the dependence of graphene Raman enhancement on the analyte concentration. We prepared Hb solutions with different concentrations: 10, 7.5, 5, 2.5, and 1 mg/mL, corresponding to 155, 116, 77, 39, and 15.5 μmol/L, respectively. Figure 3 shows the enhancement factor as a function of Hb concentration for two modes: 1376

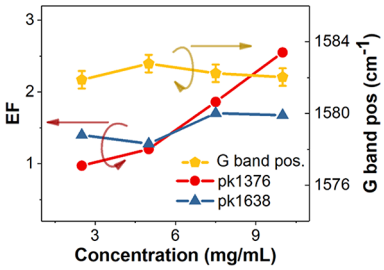

Figure 3. Dependence of Hb concentration measured with 532 nm laser. Left *Y*-axis: enhancement factor (EF) as a function of Hb concentration for two Hb Raman modes: 1376 and 1638 cm^{-1}. Right *Y*-axis: the position of graphene G band as a function of concentration. The error bars reflect the spectral resolution of the Raman spectrometer.

and 1638 cm^{-1}. We chose these two modes because they show the strongest enhancement with 532 nm excitation. It can be seen that the enhancement factor increases with increasing concentration for 1376 cm^{-1} mode. The overall trend is similar for 1638 cm^{-1} mode, except for the slightly stronger enhancement for 2.5 than 5 mg/L, and 7.5 than 10 mg/L concentrations. According to previous studies, the main mechanism for Hb adsorbed on graphene is through the heme functional group, as it has compatible molecular structure similar to hexagonal lattice of graphene.[10] The structure of heme is shown in Figure S2. Strong GERS enhancement of several heme bands, along with no observation of other modes like amide I and III bands (1656 and 1321 cm^{-1}) is indicative of an interaction between heme with graphene. In our samples, the highest GERS enhancement occurs at highest concentration implying that the molecular adsorption on graphene is not saturated. In fact, if the solution concentration is further increased, the GERS enhancement does not show any appreciable increase, due to the saturation of molecular adsorption at high concentration.[11,20] The slightly reverse trend for 1638 cm^{-1} band is possibly due to the nature of the modes: 1638 cm^{-1} mode describes the breathing distortion, while the 1376 cm^{-1} mode is the half-ring stretching mode. In our observations, the G band position of graphene is largely unchanged with different Hb concentrations, as shown in Figure 3. This suggests that the Hb solution does not dope graphene strongly, and the doping effect of different concentrations is similar. It is noted that the minimum concentration used is of the order of μMolar. Although not as low as in some other state-of-the art biosensing technologies like SPR,[4,21] SERS,[22,23] the GERS effect possesses the advantages of signal uniformity, repeatability, label-free, and low cost.

We attribute the GERS enhancement of Hb to the pi-pi interaction between graphene and Hb molecules. Graphene has pi-orbitals and the electrons in the pi-orbitals move freely and can interact with adjacent layers of graphene. GERS enhancement is mainly through chemical mechanisms, which occurs when a molecule is in direct contact with the graphene substrate.[10,20,24] The heme structure of Hb is constituted by conjugated rings, a structure that renders in achieving relatively high GERS enhancement.[10] This structure, which possess a pi-band as well, can also attach well on the graphene surface. The enhancement of heme bands rather than other types of modes confirm the interaction of heme and graphene. Due to the $\pi-\pi$ interaction between Hb and graphene, the charge transfer further facilitates the GERS enhancement.[10,17] All these effects contribute to the overall GERS enhancement.

DOI: 10.1021/acsphotonics.8b00456
ACS Photonics 2018, 5, 2978−2982

In addition to Hb, we investigated the possibility of obtaining GERS for other biomolecules, by measuring Alb in contact with graphene monolayer. Figure 4a shows the Raman

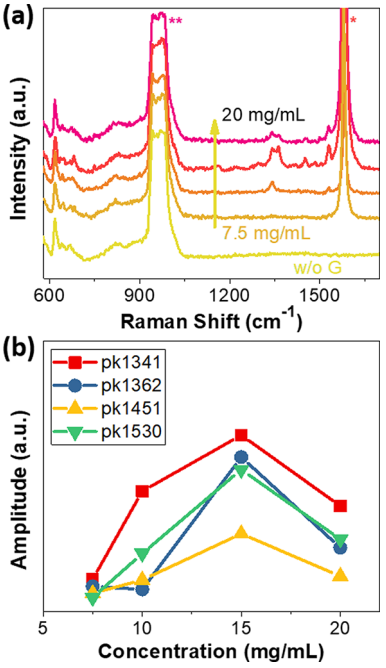

Figure 4. GERS measurement results of Alb. (a) Raman spectra of Alb on graphene (top four spectra) and w/o graphene (bottom spectrum). The spectra of Alb on graphene are from different Alb solution concentrations: 7.5, 10, 15, and 20 mg/mL from bottom to top, as illustrated in the figure. "*" shows graphene G band, and "**" shows the second-order mode of Si/SiO_2 substrate. The spectra are normalized by the Si Raman modes at 520 cm^{-1}. (b) Concentration dependence of the amplitude of four Alb Raman modes observed in experiment: 1341, 1362, 1451, and 1530 cm^{-1}. The laser power was 1 mW.

spectra of Alb with different concentrations on graphene. The Raman spectrum of only Alb without graphene on Si/SiO_2 substrate is also shown for comparison. As can be seen in the figure, under 532 nm laser excitation, Raman signal was not observable from 7.5 to 20 mg/mL concentration at 10 s integration time with 1 mW power at the sample. The power was intentionally kept low to avoid any photodegratdation of the macromolecules. The difficulty in observing clear Raman signals may be because Alb, as opposed to Hb, does not have resonance effect with 532 nm excitation. However, when Alb is placed on graphene, clear Raman signals are observed. As can be noticed in Figure 4, peaks at 1341, 1362, 1451, and 1530 cm^{-1} are clearly observed. These peaks correspond to the CH_2 twisting or CH bending, tyrosine, CH_2 and CH_3 scissoring, amide II modes of Alb molecular vibrations, respectively.[25] Akin to Hb, the GERS signal intensity of Alb is also concentration dependent. As shown in Figure 4a, the above four Raman spectra represent the concentrations 20, 15, 10, and 7.5 mg/mL, corresponding to 301, 225, 150, and 112 μM/L. The Raman peaks can be resolved in the first three concentrations, but not in the lowest one. Figure 4b summarizes the peak intensities of these concentrations. Notably, these initial results should not be interpreted as representing the lowest possible protein detection limits that are likely to be obtainable after further optimization. Some of the main advantages of using GERS for biomolecule detection are (1) signal uniformity and repeatability, in fact, our overall GERS studies on a large variety of molecules[9,10,12] show a signal variation of no more than 0.4%, (2) GERS provide fingerprint for biomolecules and thus offers high fidelity molecular information. These features make GERS a unique and appealing platform for biomedical applications.

In summary, we demonstrate for the first time, to the best of our knowledge, that Raman signal of biomolecules is enhanced when measured in contact with graphene. Our results indicate that GERS enables facile observation of Raman fingerprints of the two biomolecules, Hb and Alb, which also reveals the different attributes of biomolecules itself, such as oxidation state (e.g., ferric or ferrous heme renders frequency shift of the 1376 cm^{-1} Raman mode),[15] structure[26−28] and environment.[29,30] For the 532 nm excitation, the enhancement factor changes with different Raman modes and concentration of the solution. Interestingly, while the Raman signals of the Alb, with very low concentration and low irradiance, is not observable without graphene substrate, the Raman modes are clearly seen when the biomolecules are in contact with graphene, enabling the sensitive detection of biomolecules even in nonresonant Raman regime. The concentration dependence of GERS enhancement also reinforces the fact that GERS occurs when specific functional groups of the biomolecule interacts with graphene surface. The analysis of mode enhancement reveals that the enhancement is through the direct contact involving $\pi-\pi$ interaction between graphene and biomolecules. This work paves a new avenue for biosensing using GERS, which shows great potential as a simple, nondestructive, reliable and inexpensive platform with ubiquitous sensing capabilities.

■ ASSOCIATED CONTENT

Supporting Information

The Supporting Information is available free of charge on the ACS Publications website at DOI: 10.1021/acsphotonics.8b00456.

Experimental methods on sample preparation and Raman measurement; discussions on the graphene quality; choice of monolayer graphene; interference effect on SiO_2/Si substrate; GERS enhancement for different molecules and on different thicknesses of graphene; figures of Raman and AFM of graphene flakes; structures of Hb and Alb; illustration of exfoliation process; Raman spectra of glue residue; Raman spectra of Hb on monolayer and multilayer graphene; tables of the GERS enhancement factor on a number of other organic molecules; calculated reflection of monolayer graphene on SiO_2/Si substrate and only SiO_2/Si (PDF).

■ AUTHOR INFORMATION

Corresponding Authors

*E-mail: sjh5899@psu.edu.
*E-mail: pandey@uchc.edu.
*E-mail: jingkong@mit.edu.

ORCID

Shengxi Huang: 0000-0002-3618-9074
Ishan Barman: 0000-0003-0800-0825
Jing Kong: 0000-0003-0551-1208

DOI: 10.1021/acsphotonics.8b00456
ACS Photonics 2018, 5, 2978−2982

Author Contributions

[#]These authors contributed equally to this work.

Author Contributions

S.H. and R.P. designed and performed the experiment and analyzed the results. J.K. and M.D. supervised the work. All authors discussed the results and contributed in writing the manuscript.

Notes

The authors declare no competing financial interest.

■ ACKNOWLEDGMENTS

S.H., J.K., and M.D. acknowledge the NSF Grant EFRI 2-DARE(EFMA-1542815).

■ REFERENCES

(1) Tabata, M.; Goda, T.; Matsumoto, A.; Miyahara, Y. Field-Effect Transistors for Detection of Biomolecular Recognition. *Intelligent Nanosystems for Energy, Information and Biological Technologies*; Springer: Tokyo, Japan, 2016; pp 13−25.

(2) Wang, J. Electrochemical Glucose Biosensors. *Chem. Rev.* **2008**, *108* (2), 814−825.

(3) Pandey, R.; Paidi, S. K.; Valdez, T. A.; Zhang, C.; Spegazzini, N.; Dasari, R. R.; Barman, I. Noninvasive Monitoring of Blood Glucose with Raman Spectroscopy. *Acc. Chem. Res.* **2017**, *50* (2), 264−272.

(4) Piliarik, M.; Vaisocherová, H.; Homola, J. *Surface Plasmon Resonance Biosensing*; Humana Press, 2009; pp 65−88.

(5) Kneipp, K.; Wang, Y.; Kneipp, H.; Perelman, L. T.; Itzkan, I.; Dasari, R. R.; Feld, M. S. Single Molecule Detection Using Surface-Enhanced Raman Scattering (SERS). *Phys. Rev. Lett.* **1997**, *78* (9), 1667−1670.

(6) Nie, S. Probing Single Molecules and Single Nanoparticles by Surface-Enhanced Raman Scattering. *Science (Washington, DC, U. S.)* **1997**, *275* (5303), 1102−1106.

(7) Creighton, J. A.; Blatchford, C. G.; Albrecht, M. G. Plasma Resonance Enhancement of Raman Scattering by Pyridine Adsorbed on Silver or Gold Sol Particles of Size Comparable to the Excitation Wavelength. *J. Chem. Soc., Faraday Trans. 2* **1979**, *75*, 790.

(8) Natan, M. J. Concluding Remarks: Surface Enhanced Raman Scattering. *Faraday Discuss.* **2006**, *132*, 321.

(9) Ling, X.; Huang, S.; Deng, S.; Mao, N.; Kong, J.; Dresselhaus, M. S.; Zhang, J. Lighting Up the Raman Signal of Molecules in the Vicinity of Graphene Related Materials. *Acc. Chem. Res.* **2015**, *48* (7), 1862−1870.

(10) Huang, S.; Ling, X.; Liang, L.; Song, Y.; Fang, W.; Zhang, J.; Kong, J.; Meunier, V.; Dresselhaus, M. S. Molecular Selectivity of Graphene-Enhanced Raman Scattering. *Nano Lett.* **2015**, *15* (5), 2892−2901.

(11) Ling, X.; Xie, L.; Fang, Y.; Xu, H.; Zhang, H.; Kong, J.; Dresselhaus, M. S.; Zhang, J.; Liu, Z. Can Graphene Be Used as a Substrate for Raman Enhancement? *Nano Lett.* **2010**, *10* (2), 553−561.

(12) Ling, X.; Huang, S.; Kong, J.; Dresselhaus, M. Graphene-Enhanced Raman Scattering (GERS): Chemical Effect. *Recent Developments in Plasmon-Supported Raman Spectroscopy*; World Scientific (Europe), 2018; pp 415−449.

(13) Lin, J.; Zhang, N.; Tong, L.; Zhang, J. *ACS Symp. Ser.* **2016**, *1246*, 97−119.

(14) Xie, L.; Ling, X.; Fang, Y.; Zhang, J.; Liu, Z. Graphene as a Substrate To Suppress Fluorescence in Resonance Raman Spectroscopy. *J. Am. Chem. Soc.* **2009**, *131* (29), 9890−9891.

(15) Wood, B. R.; Asghari-Khiavi, M.; Bailo, E.; McNaughton, D.; Deckert, V. Detection of Nano-Oxidation Sites on the Surface of Hemoglobin Crystals Using Tip-Enhanced Raman Scattering. *Nano Lett.* **2012**, *12* (3), 1555−1560.

(16) Hobro, A. J.; Konishi, A.; Coban, C.; Smith, N. I.; Ohata, K.; Aoshi, T.; Itagaki, S.; Sato, S.; Narita, H.; Abdelgelil, N. H.; Inoue, M.; Culleton, R.; Kaneko, O.; Nakagawa, A.; Horii, T.; Akira, S.; Ishii, K. J.; Coban, C. Raman Spectroscopic Analysis of Malaria Disease Progression via Blood and Plasma Samples. *Analyst* **2013**, *138* (14), 3927.

(17) Ling, X.; Moura, L. G.; Pimenta, M. A.; Zhang, J. Charge-Transfer Mechanism in Graphene-Enhanced Raman Scattering. *J. Phys. Chem. C* **2012**, *116* (47), 25112−25118.

(18) Ling, X.; Fang, W.; Lee, Y.-H.; Araujo, P. T.; Zhang, X.; Rodriguez-Nieva, J. F.; Lin, Y.; Zhang, J.; Kong, J.; Dresselhaus, M. S. Raman Enhancement Effect on Two-Dimensional Layered Materials: Graphene, h-BN and MoS2. *Nano Lett.* **2014**, *14* (6), 3033−3040.

(19) Barros, E. B.; Dresselhaus, M. S. Theory of Raman Enhancement by Two-Dimensional Materials: Applications for Graphene-Enhanced Raman Spectroscopy. *Phys. Rev. B: Condens. Matter Mater. Phys.* **2014**, *90* (3), 035443.

(20) Ling, X.; Zhang, J. First-Layer Effect in Graphene-Enhanced Raman Scattering. *Small* **2010**, *6* (18), 2020−2025.

(21) Liu, Y.; Liu, Q.; Chen, S.; Cheng, F.; Wang, H.; Peng, W. Surface Plasmon Resonance Biosensor Based on Smart Phone Platforms. *Sci. Rep.* **2015**, *5* (1), 12864.

(22) Michaels, A. M.; Nirmal, M.; Brus, L. E. Surface Enhanced Raman Spectroscopy of Individual Rhodamine 6G Molecules on Large Ag Nanocrystals. *J. Am. Chem. Soc.* **1999**, *121* (43), 9932−9939.

(23) Kneipp, K.; Kneipp, H.; Itzkan, I.; Dasari, R. R.; Feld, M. S. Ultrasensitive Chemical Analysis by Raman Spectroscopy. *Chem. Rev.* **1999**, *99* (10), 2957−2976.

(24) Otto, A.; Futamata, M. Electronic Mechanisms of SERS. *Top. Appl. Phys.* **2006**, *103*, 147−182.

(25) Fazio, B.; D'Andrea, C.; Foti, A.; Messina, E.; Irrera, A.; Donato, M. G.; Villari, V.; Micali, N.; Maragò, O. M.; Gucciardi, P. G. SERS Detection of Biomolecules at Physiological PH via Aggregation of Gold Nanorods Mediated by Optical Forces and Plasmonic Heating. *Sci. Rep.* **2016**, *6* (1), 26952.

(26) Chi, Z.; Chen, X. G.; Holtz, J. S. W.; Asher, S. A. UV Resonance Raman-Selective Amide Vibrational Enhancement: Quantitative Methodology for Determining Protein Secondary Structure †. *Biochemistry* **1998**, *37* (9), 2854−2864.

(27) Svetlakova, A. S.; Brandt, N. N.; Priezzhev, A. V.; Chikishev, A. Y. Raman Microspectroscopy of Nanodiamond-Induced Structural Changes in Albumin. *J. Biomed. Opt.* **2015**, *20* (4), 047004.

(28) Peng, X.; Yao, D.; Pan, Y.; Yu, Q.; Ni, S.; Bian, H.; Huang, F.; Liang, H. Study on the Structural Changes of Bovine Serum Albumin with Effects on Polydatin Binding by a Multitechnique Approach. *Spectrochim. Acta, Part A* **2011**, *81* (1), 209−214.

(29) Tu, Q.; Chang, C. Diagnostic Applications of Raman Spectroscopy. *Nanomedicine* **2012**, *8* (5), 545−558.

(30) Hanlon, E. B.; Manoharan, R.; Koo, T.-W.; Shafer, K. E.; Motz, J. T.; Fitzmaurice, M.; Kramer, J. R.; Itzkan, I.; Dasari, R. R.; Feld, M. S. Prospects for *in Vivo* Raman Spectroscopy. *Phys. Med. Biol.* **2000**, *45* (2), R1−R59.

DOI: 10.1021/acsphotonics.8b00456
ACS Photonics 2018, 5, 2978−2982